Supporting Information

Molecular Behavior of Silicone Adhesive at Buried Polymer Interface Studied by Molecular Dynamics Simulation and Sum Frequency Generation Vibrational Spectroscopy

Yuchen Wu,[1,2] Ting Lin,[1,2] Elizabeth Santos,[3] Dongchan Ahn,[3] Ryan Marson,[3] Pranab Sarker,[4,5] Xiaoyun Chen,[3] Frédéric Gubbels, [3] Nick E. Shephard,[3] Carol Mohler,[3] Tao Wei,[4,5,*] Tzu-Chi Kuo,[3] Zhan Chen[1,2,*]

[1]Department of Chemistry, [2]Department of Macromolecular Science and Engineering, University of Michigan, MI 48109
[3]The Dow Chemical Company, Midland, MI 48674
[4]Department of Biomedical Engineering, [5]Department of Chemical Engineering, University of South Carolina, Columbia, SC 29208

*Corresponding Authors: Zhan Chen, zhanc@umich.edu; Tao Wei, TAOW@mailbox.sc.edu

Table of Content

S1 Methodology

Umbrella sampling

The umbrella sampling method was used to obtain the free energy of the system when a (3-glycidoxypropyl)trimethoxy silane (γ-GPS) molecule was at different locations of the simulation box. Using this method, a γ-GPS molecule at the interface was randomly chosen to move along the Z-axis to go through the interface. It was gradually pulled up along the Z-axis by 2 nm, starting from its initial position. With every 0.1 nm, the system was simulated to reach equilibrium, and then the final configuration of the sample system was chosen for analysis. Similarly, the γ-GPS molecule was pulled downward along the Z-axis by 2 nm (0.1 nm for each step). During the relaxation, the chosen γ-GPS molecule was constrained to its original place in the center of the window with a harmonic potential represented by

$$u_i(Z_i) = \frac{1}{2}k'(Z_{com} - Z_i)^2 \tag{1}$$

where k′ is the force constant, Z_{com} is the Z coordinate of the chosen molecule's center of the mass, Z_i is the center position of the ith window (or step), and u_i (Z_i) is the corresponding harmonic potential. To make sure the total number of windows is sufficient and all the windows are overlapped well, $k = 3000$ kJ mol^{-1} Å^{-2} was chosen. To ensure a smooth connection between both PMF profiles for upward and downward pulling, we selected a central window as the starting point (i.e., the initial window) for reference. Correspondingly, the PMF value at this initial point was set to zero. For each configuration, we performed simulations to relax the system to reach equilibrium or a "final" state. We then calculated the potential of mean force (PMF) using the reference location at the PET/PDMS interface. In the simulation, the weighted histogram analysis (WHAM)[1] was used to calculate PMF.

Atomistic MD simulations and free energy computation

In this study, we used atomic MD simulation and free energy perturbation to investigate how the free energy of the system changes with different orientations. Using this method, we could deduce the most likely orientation of the γ-GPS molecule at the interface. Solvation free energies (ΔF) were calculated using the method of alchemical free energy perturbation (FEP)[2,3].

For each system, we have used twenty different discrete values of λ in two separate sets. The first set of ten discrete λ values was used to control Lennard-Jones (LJ) interactions between the solute and its environment, while the second set of ten discrete λ values was used to modify the solute charges. To avoid end-point catastrophe and numerical issues while computing the solute-solvent interactions in the free energy calculations, the non-linear soft-core scheme was adopted.

### *Estimation of partial charges of γ-GPS and DMMVS for MD simulations*

The partial charges for γ-GPS and DMMVS were obtained following the protocols outlined in our previous work[4,5] within the restrained ESP or RESP-AMBER fitting procedure[6]. The Hartree-Fock *ab initio* method with a 6-31* basis set, as suggested in the AMBER protocol, was employed to estimate the electrostatic potentials (ESP) of the gas-phase zwitterions. Those ESP data were then fed into RESP-AMBER fitting procedure to calculate the partial charges. Before calculating the ESPs of γ-GPS and DMMVS, their geometries were optimized within the DFT framework. The B3YLP function with 6-311G (2d, p) basis set and D3 version of Grimme's dispersion with Becke-Johnson damping (GD3BJ)[7] were used. Gaussian16[8] package was utilized for both optimization and ESP calculation.

Partial charges of the molecules

The partial charges of atoms of γ-GPS, DMMVS, PET, PDMS matrix and PDMS cross-

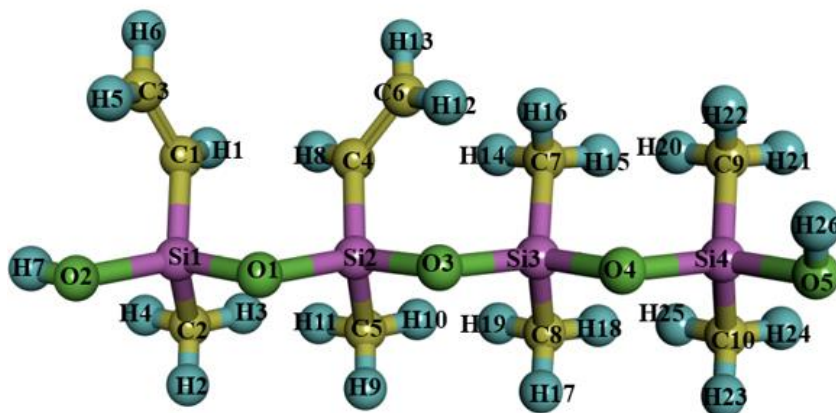linker are listed in the Figure S1, Figure S2, Figure S3, and Figure S4 respectively.

a)

b)
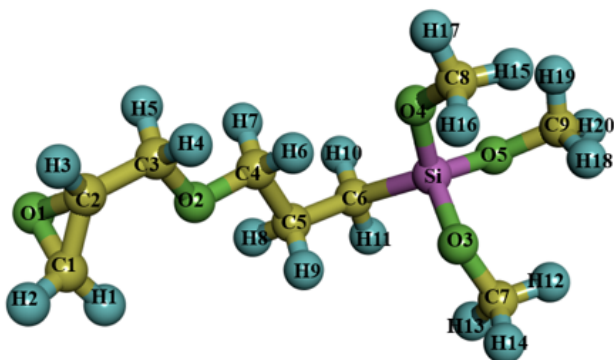
Atoms	Labels	Charge
Si	Si	1.2042
O	O1	-0.2266
	O2	-0.2266
	O3, O4, O5	-0.4558
C	C1	0.0073
	C2	0.0603
	C3	0.0073
	C4	0.0073
	C5	-0.1060
	C6	-0.2827
	C7, C8, C9	-0.0457
H	H1 - H20	0.0530

Figure S1. (a) The molecular structure of γ-GPS molecule. (b) The partial charges of γ-GPS molecule.

a)

b)

Atoms	Labels	Charge
Si	Si1 - Si4	1.3810
O	O1	-0.8300
	O2	-0.8500
	O3	-0.8300
	O4	-0.8300
	O5	-0.8500
C	C1	-0.8270
	C2	-0.4780
	C3	0.0930
	C4	-0.8270
	C5	-0.4780
	C6	0.0900
	C7 - C10	-0.7580
H	H1	0.2840
	H2 - H4	0.0900
	H5 - H6	0.0520
	H7	0.4550
	H8	0.2840
	H9 - H11	0.0900
	H12 - H13	0.0520
	H14 - H25	0.1590
	H26	0.4460

Figure S2. (a) The molecular structure of DMMVS molecule. (b) The partial charges of DMMVS molecule.

PET Part 1

a)

b)

Atoms	Labels	Charge
O	O1	-0.3964
	O2	-0.1163
	O3	-0.1163
	O4	-0.3964
	O5	-0.5374
C	C1	0.4644
	C2 - C3	-0.1305
	C4	-0.0650
	C5 - C6	-0.1305
	C7	-0.0650
	C8	0.4644
	C9 - C10	0.0073
H	H1 - H4	0.1305
	H5 - H8	0.0530
	H9	0.4241

PET Part 2

c)

d)

Atoms	Labels	Charge
O	O1	-0.3964
	O2	-0.1163
	O3	-0.1163
	O4	-0.3964
C	C1	0.4644
	C2 - C3	-0.1305
	C4	-0.0650
	C5 - C6	-0.1305
	C7	-0.0650
	C8	0.4644
	C9 - C10	0.0073
H	H1 - H4	0.1305
	H5 - H8	0.0530

PET Part 3

e)

f)

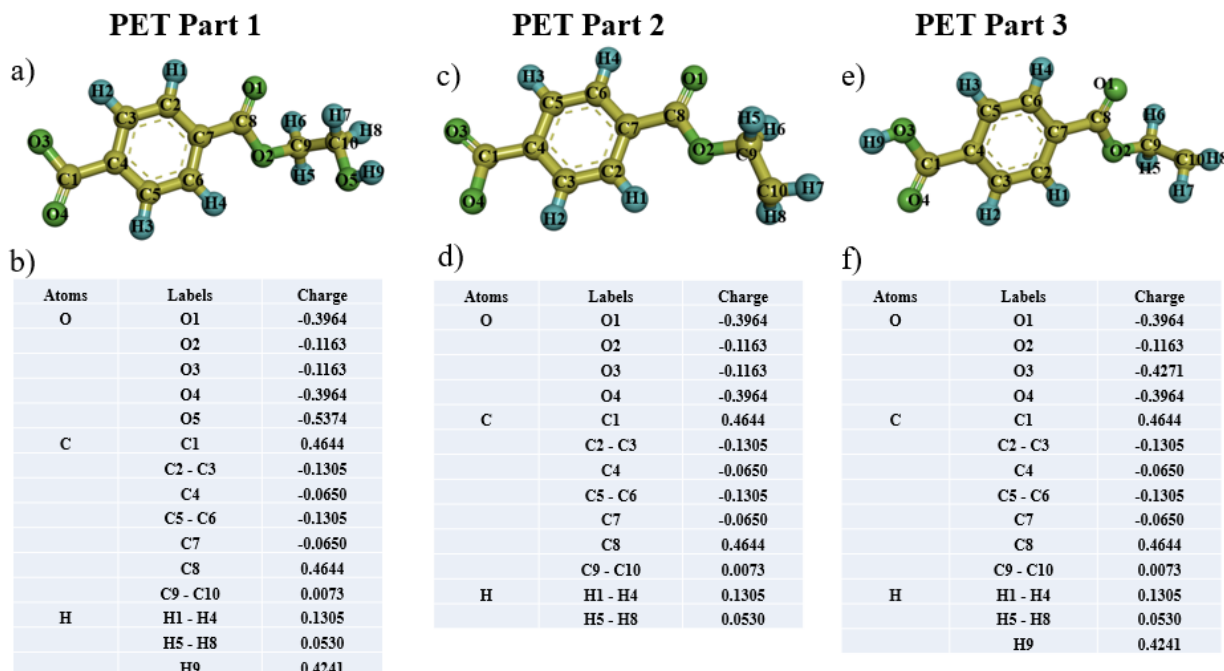| Atoms	Labels	Charge
O	O1	-0.3964
	O2	-0.1163
	O3	-0.4271
	O4	-0.3964
C	C1	0.4644
	C2 - C3	-0.1305
	C4	-0.0650
	C5 - C6	-0.1305
	C7	-0.0650
	C8	0.4644
	C9 - C10	0.0073
H	H1 - H4	0.1305
	H5 - H8	0.0530
	H9	0.4241

Figure S3. The molecular structure of PET molecule. PET molecule was divided into three parts. Head part: PET Part 1 (a), middle part or repeating unit: PET Part 2 (c), tail part: PET Part 3 (e). The partial charges of PET molecule for PET Part 1 (b), PET Part 2 (d) and PET Part 3 (f).
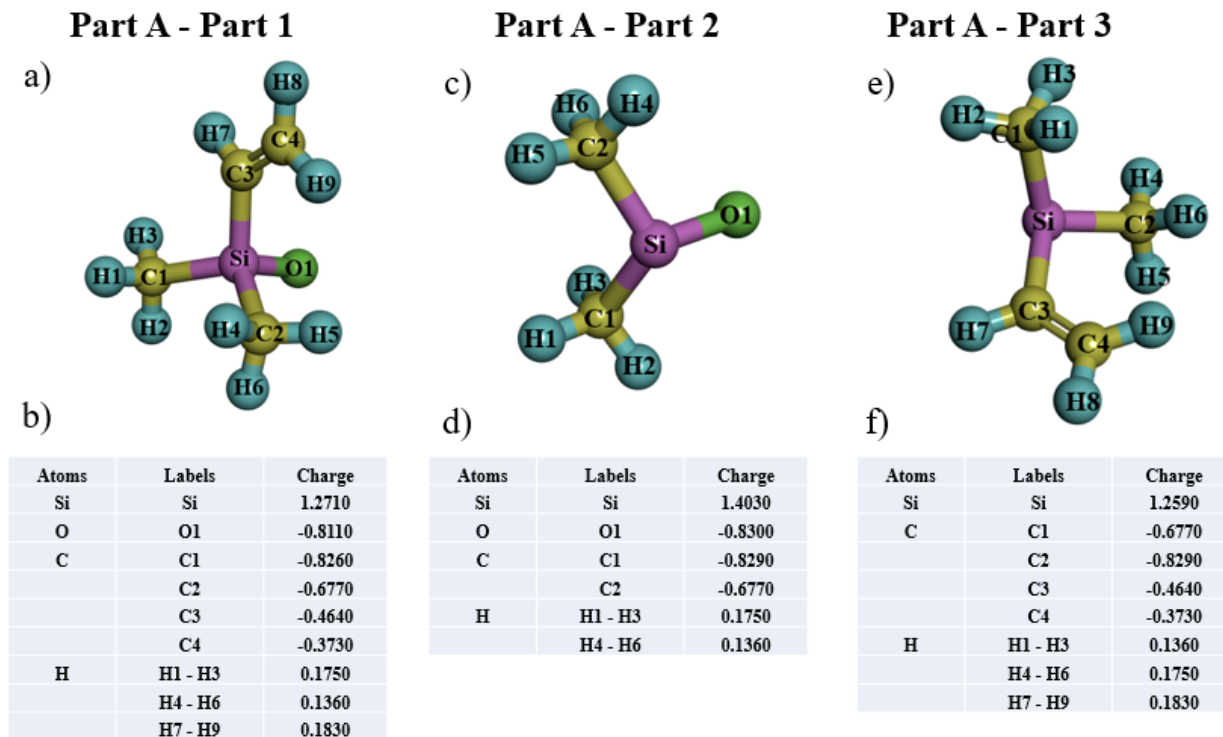
Part A - Part 1

a)

b)

Atoms	Labels	Charge
Si	Si	1.2710
O	O1	-0.8110
C	C1	-0.8260
	C2	-0.6770
	C3	-0.4640
	C4	-0.3730
H	H1 - H3	0.1750
	H4 - H6	0.1360
	H7 - H9	0.1830

Part A - Part 2

c)

d)

Atoms	Labels	Charge
Si	Si	1.4030
O	O1	-0.8300
C	C1	-0.8290
	C2	-0.6770
H	H1 - H3	0.1750
	H4 - H6	0.1360

Part A - Part 3

e)

f)

Atoms	Labels	Charge
Si	Si	1.2590
C	C1	-0.6770
	C2	-0.8290
	C3	-0.4640
	C4	-0.3730
H	H1 - H3	0.1360
	H4 - H6	0.1750
	H7 - H9	0.1830

Figure S4. The molecular structure of PDMS Part A. Part A molecule was divided into three parts. Head part: Part A - Part 1 (a), middle part or repeating unit: Part A - Part 2 (c), tail part: Part A -

Part 3 (e). The partial charges of Part A molecule for Part A – Part 1 (b), Part A - Part 2 (d), Part A - Part 3 (f).
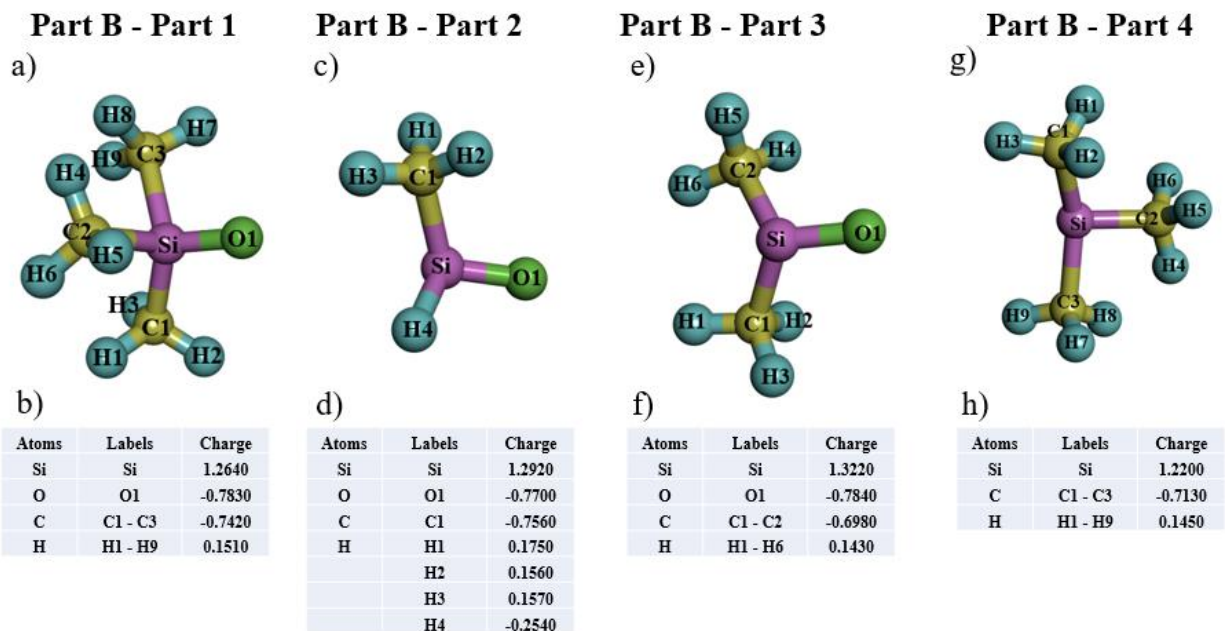
Part B - Part 1

a)

Part B - Part 2

c)

Part B - Part 3

e)

Part B - Part 4

g)

b)

Atoms	Labels	Charge
Si	Si	1.2640
O	O1	-0.7830
C	C1 - C3	-0.7420
H	H1 - H9	0.1510

d)

Atoms	Labels	Charge
Si	Si	1.2920
O	O1	-0.7700
C	C1	-0.7560
H	H1	0.1750
	H2	0.1560
	H3	0.1570
	H4	-0.2540

f)

Atoms	Labels	Charge
Si	Si	1.3220
O	O1	-0.7840
C	C1 - C2	-0.6980
H	H1 - H6	0.1430

h)

Atoms	Labels	Charge
Si	Si	1.2200
C	C1 - C3	-0.7130
H	H1 - H9	0.1450

Figure S5. The molecular structure of PDMS Part B. Part B molecule was divided into four parts. Head part: Part B - Part 1 (a), middle part or repeating unit: Part B - Part 2 (c) and Part B - Part 3 (e), tail part: Part B - Part 4 (g). The partial charges of Part B molecule for Part B - Part 1 (b), Part B - Part 2 (d), Part B - Part 3 (f), Part B - Part 4 (h),

S2. Crystallinity formation during the atomistic MD simulation

Figures S6a, 6b, and 6c show the initial, the middle and the final configurations of the three-layer system. In the initial structure, shown in Figure S6a, there was no PET crystal in the box. After 300-ns MD simulation at 500K, the crystal structure showed up in the PET layer (Figure S6b). In the final configuration, shown in Figure S6c, the PET crystalized domain grew even larger in the PET layer. Comparing three figures, we found that the PET crystal gradually formed and grew larger during the MD simulation. Here the simulation was conducted at 500 K for more than 800 ns, while 500K is between the glass transition temperature (350K) and the melting temperature (533.1K) of PET. Therefore, the temperature condition in the simulation is suitable for PET to form crystal structure.
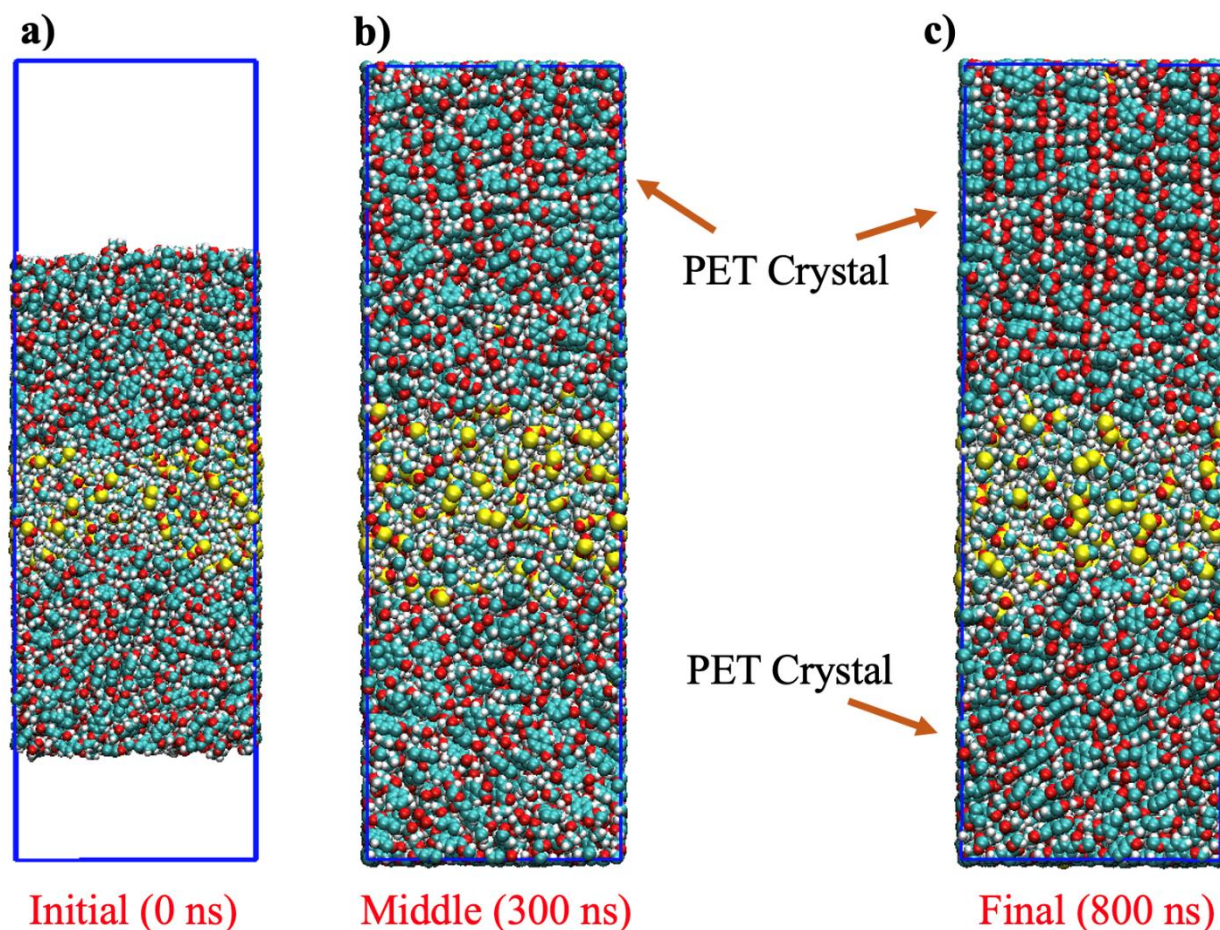
Figure S6. Configurations of the three-layer system at different simulation times. (a) The initial configuration (0 ns), (b) the middle configuration (300 ns), and (c) the final configuration (800 ns) of the three-layer system. Note: The initial configuration is the configuration before NPT MD simulation. The vacuum at the top and the bottom was created to prevent PBC conditions. After NPT MD simulation the vacuum disappeared, shown in Figures S6b and S6c.

References:

(1) Kumar, S.; Rosenberg, J. M.; Bouzida, D.; Swendsen, R. H.; Kollman, P. A. The Weighted Histogram Analysis Method for Free-energy Calculations on Biomolecules. I. The Method. *J Comput Chem* **1992**, *13* (8), 1011–1021. https://doi.org/10.1002/jcc.540130812.

(2) Wyczalkowski, M. A.; Vitalis, A.; Pappu, R. V. New Estimators for Calculating Solvation Entropy and Enthalpy and Comparative Assessments of Their Accuracy and Precision. *J. Phys. Chem. B* **2010**, *114* (24), 8166–8180. https://doi.org/10.1021/jp103050u.

(3) Shirts, M. R.; Mobley, D. L.; Chodera, J. D. Chapter 4 Alchemical Free Energy Calculations: Ready for Prime Time? In *Annual Reports in Computational Chemistry*; Elsevier, 2007; Vol. 3, pp 41–59. https://doi.org/10.1016/S1574-1400(07)03004-6.

(4) Sarker, P.; Lu, T.; Liu, D.; Wu, G.; Chen, H.; Jahan Sajib, M. S.; Jiang, S.; Chen, Z.; Wei, T. Hydration Behaviors of Nonfouling Zwitterionic Materials. *Chem. Sci.* **2023**, *14* (27), 7500–

7511. https://doi.org/10.1039/D3SC01977B.

(5) Huang, H.; Zhang, C.; Crisci, R.; Lu, T.; Hung, H.-C.; Sajib, M. S. J.; Sarker, P.; Ma, J.; Wei, T.; Jiang, S.; Chen, Z. Strong Surface Hydration and Salt Resistant Mechanism of a New Nonfouling Zwitterionic Polymer Based on Protein Stabilizer TMAO. *J. Am. Chem. Soc.* **2021**, *143* (40), 16786–16795. https://doi.org/10.1021/jacs.1c08280.

(6) Bayly, C. I.; Cieplak, P.; Cornell, W.; Kollman, P. A. A Well-Behaved Electrostatic Potential Based Method Using Charge Restraints for Deriving Atomic Charges: The RESP Model. *J. Phys. Chem.* **1993**, *97* (40), 10269–10280. https://doi.org/10.1021/j100142a004.

(7) Grimme, S.; Ehrlich, S.; Goerigk, L. Effect of the Damping Function in Dispersion Corrected Density Functional Theory. *J Comput Chem* **2011**, *32* (7), 1456–1465. https://doi.org/10.1002/jcc.21759.

(8) Kulsha, A. V.; Sharapa, D. I. Superhalogen and Superacid. *J Comput Chem* **2019**, *40* (26), 2293–2300. https://doi.org/10.1002/jcc.26007.